Наносистеми, наноматеріали, нанотехнології
Nanosistemi, Nanomateriali, Nanotehnologii
2021, т. 19, № 4, сс. 855–863

PACS numbers: 61.05.cp, 68.37.Hk, 78.30.Hv, 78.67.Bf, 81.07.Bc, 81.16.Hc, 81.70.Pg

Preparation and Characterization of Zinc Oxide Nanoparticles *via* the Thermal Decomposition

Douaa Alhaddad[1], Farouk Kndil[1], and Ahmad Falah[1,2]

[1]*Department of Chemistry,*
Damascus University,
Mousalam Baroudy Str.,
Damascus, Syria
[2]*Faculty of Pharmacy,*
Arab International University (AIU),
Al-Mazzeh Highway,
Damascus, Syria

Zinc oxide nanoparticles are successfully synthesized *via* a thermal decomposition of the Schiff base complexes [(bis-N-(4-metoxy-benzylidene)-2-nitro-1,4 diaminobenzene) Zn(II)], [D1, Zn(II)] as precursor *via* calcification at the temperature of 600°C for 3 hours in an electrical furnace and the air in the presence of non-ionic surfactant [secondary alcohol ethoxylate (TERGITOL™ 15-S-40 (70%)] and polymer polyvinylpyrrolidone (PVP). ZnO nanoparticles are obtained with average size of the crystals of 36.8 nm. The as-synthesized products are characterized by powder x-ray diffraction (XRD), scanning electron microscopy (SEM), Fourier transform infrared spectroscopy (FT-IR); elemental analysis of the particles is performed by energy dispersive x-ray spectroscopy (EDX).

Наночастинки оксиду Цинку успішно синтезуються за допомогою теплового розкладання комплексів Шиффових основ [(біс-N-(4-метоксі-бензиліден)-2-нітро-1,4 діамінобензол) цинк(II)], [D1, Zn(II)] як провісника через кальцифікацію за температури у 600°C протягом 3 годин в електричній печі та повітрі в присутності нейонної поверхнево-активної речовини [вторинний спиртовий етоксилат (TERGITOL™ 15-S-40 (70%)] і полімерний полівінілпірролідон (ПВП). Наночастинки ZnO одержують із середнім розміром кристалів у 36,8 нм. Щойно синтезовані продукти характеризуються порошковою рентґенівською дифракцією (XRD), сканувальною електронною мікроскопією (SEM), інфрачервоною спектроскопією на основі перетвору Фур'є (FT-IR); елементна аналіза частинок проводиться за допомогою рентґеноспектральної спектроскопії на основі методи енергетичної дисперсії (EDX).

Key words: thermal decomposition, Schiff base complexes, Zinc oxide nanoparticles, Schiff bases of *p*-anisaldehyde.

Ключові слова: термічне розкладання, комплекси Шиффових основ, наночастинки оксиду Цинку, Шиффові основи *p*-анісового альдегіду.

(Received 14 December, 2020; in revised form, 19 December, 2021)

1. INTRODUCTION

Recently, syntheses of materials of nanosizes have attracted attentions attributed to their unique mechanical, physical, optical, and magnetic properties [1]. The properties of nanomaterials stimulate various applications in different technological fields such as electronics, catalysis, magnetic data storage, energy storage, structural components, and ceramics [2]. Among inorganic material, Zinc oxide (ZnO) [3] is semiconducting material with direct band gap of 3.3 eV at room temperature and with unique properties such as optical transparency, electric conductivity, piezoelectricity and near-UV emission [4]. This metal oxide has a variety of applications including chemical sensors [5], catalysts [6], UV light-emitters [7], photovoltaics [8], and cantilevers [9]. Several approaches have been engaged to synthesize ZnO nanocrystals such as thermal methods [10], electrochemical methods [11], sol–gel methods [12], solid-state reactions [13], chemical reduction and decomposition route [14], sonochemical methods [15]. Most of these approaches require tedious processes, expensive substrates, sophisticated equipment and rigorous experimental circumstances. Recently, metal oxides' nanoparticles have been synthesized *via* thermal decomposition method of Schiff base complexes [16] that returns to this method not only avoided usage of the template and complex apparatus, but also affectivity in the shape control of the preparation product. By selecting a proper precursor with a rational calcining procedure, products with unique size and shapes could be obtained. This method also has extra advantages, including operational simplicity, high purity and high yield of product, low-energy consumption and no special equipment required [17]. However, in this work, ZnO nanoparticles have been synthesized *via* thermal decomposition of Schiff base complexes [D1, Zn(II)] as precursor by calcification in electrical furnace with non-ionic surfactant and polymer polyvinylpyrrolidone (PVP).

2. EXPERIMENTAL PROCEDURE

2.1. Materials

Zinc nitrate 6-hydrat (10196-18-6), ethanol solution (16368), 2-nitro-1,4-phenylenediamine (N21200), *p*-anisaldehyde (A88107), non-ionic

surfactant [secondary alcohol ethoxylate (TERGITOL™ 15-S-40 (70%)] (STS0003) and polymer polyvinylpyrrolidone (PVP40), all the chemical reagents, were obtained from Sigma-Aldrich.

2.2. Preparation Ligand [Bis-N-(4-Metoxy-Benzylidene)-2-Nitro-1,4 Diaminobenzene]

The symmetrical Schiff base (D1) was prepared by refluxing (0.05 mole) of *p*-anisaldehyde and (0.025 mole) of 2-nitro-1,4-phenylene-diamine in (30 ml) of dried ethanol for 4 h and cooling the reaction mixture. The Schiff base was separated as orange needles and was recrystallized twice from methanol (yield 90%). The compound is stable at room temperature.

Figure 1 shows the chemical preparation of ligand (D1):

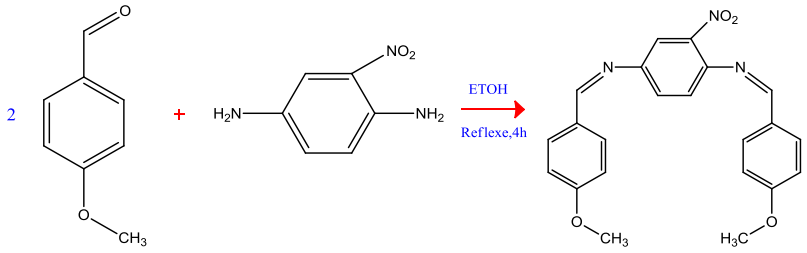

Fig. 1.

2.3. Preparation of [D1, Zn(II)] Complex

Ligand D1 (2 mmole) was dissolved in 15 mL of ethanol, mixed with $Zn(NO_3)_2 \cdot 6H_2O$ (2 mmole, in ethanol) at 100°C and stirred for 2 h. The dark orange precipitates were washed several times using distilled water and dried in the air.

2.5. Synthesis of ZnO Nanoparticles

Ligand D1 (2 mmole) was dissolved in 15 ml of ethanol, mixed with $Zn(NO_3)_2 \cdot 6H_2O$ (2 mmole, in ethanol) at 100°C and stirred for 30 min. Then, we added 7 gr of non-ionic surfactant and stirred continuously for 1 h. Finally, we add 3 gr of polymer polyvinylpyrrolidone (PVP). ZnO nanocrystals were produced by subjecting the previous prepared complex [D1, Zn(II)] to thermal treatment at a relatively low temperature (600°C) in the air, and after keeping the thermal treatment at 600°C for 3 h. The white nanocrystals of ZnO were cooled at room temperature, and then washed with ethanol and distilled water for three times and dried in the air.

3. RESULTS AND DISCUSSION

3.1. Characterization by Using FT-IR Spectroscopy

Compounds have been clearly characterized by using Fourier transform infrared spectroscopy (FT-IR). The structure of Schiff base ligand was confirmed with disappearance of the amine and aldehyde group and in the oxides; the corresponding peaks appeared in Fig. 2, *a* show FT-IR spectra of the precursors. Characteristic peaks at 1.635 cm^{-1} are attributed to the C=N stretching, and 1560, 1348 cm^{-1} belongs to nitrogroup NO_2. The strong broad peak around 3463 cm^{-1} belongs to N–H group as result of tautomeric isomerism, and at 3136 cm^{-1}, due to aromatic C–H.

FT-IR spectra of prepared nanoparticles are given in Fig. 2, *b*. Strong broad peak around 479 cm^{-1} shows a distinct stretching mode of ZnO crystal. The broad absorption band of O–H stretching ($\cong$ 3500 cm^{-1}) is due to adsorbed water on the external surface of the samples during handling to record the spectra.

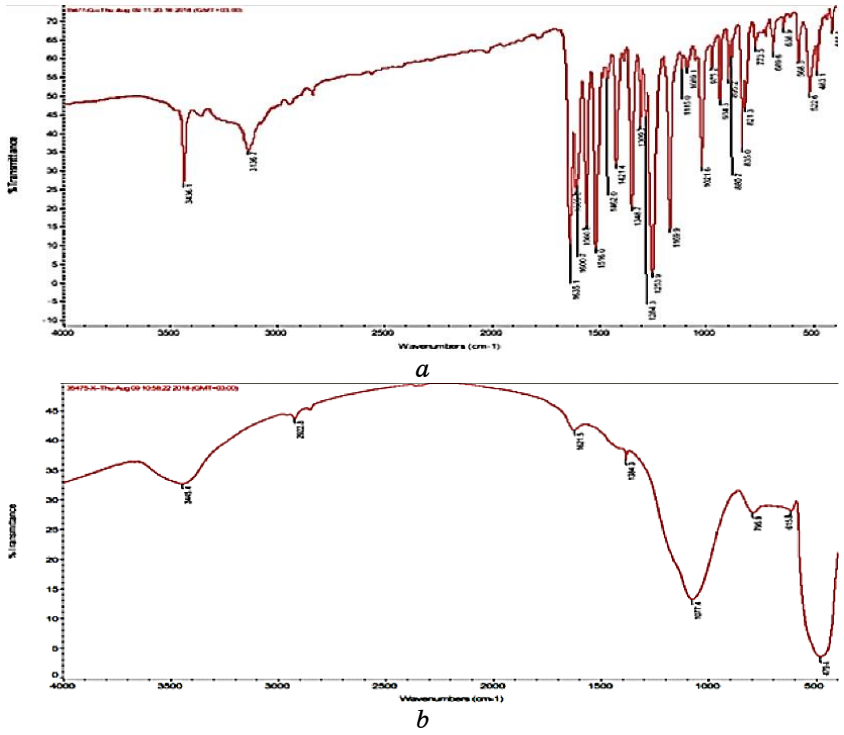

Fig. 2. FT-IR spectra of Schiff base ligand [D1] (*a*); FT-IR spectra of ZnO nanoparticles (*b*).

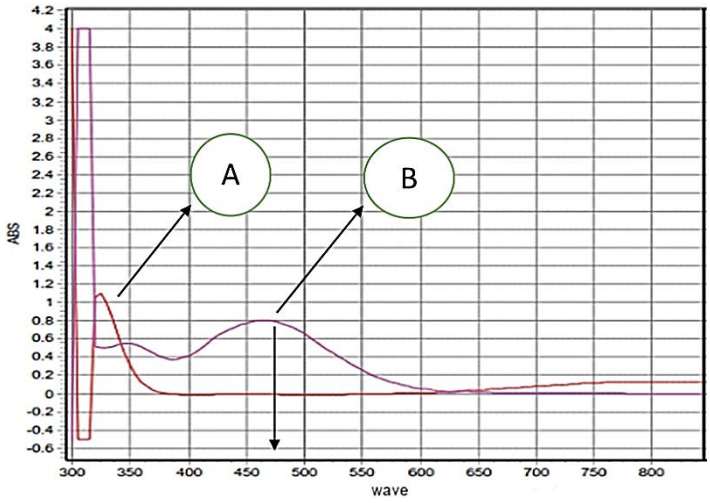

Fig. 3. Line (A)—UV-vis spectra for Schiff base ligand [D1]; line (B)—UV-vis spectra for [D1, Zn (II)] complex.

3.2. UV-Vis Spectroscopy

The complexes have been confirmed by UV-vis spectroscopy, which show shifts in the absorption peaks between ligand and their complexes because of differences in electronic transitions.

In Figure 3, there are line (A) of UV-vis spectra of Schiff base ligand [D1], and line (B), *i.e.*, line (A) for [D1, Zn(II)] complex. The ligand displays typical ligand-centred $\pi \rightarrow \pi^*$-transitions at 325 nm. Upon co-ordination with Zinc ions, there are minor changes of these bands. The visible spectra of complexes are clearly shown with line (B); for Zn(II) complex, absorption appears at 465 nm, and they can be assigned to $d \rightarrow d$-electron transition or metal to ligand charge transfer (MLCT).

3.3. Thermogravimetric Analysis of the Schiff Base Complexes

In Figure 4, the thermal behaviour of Zn(II) complex has been studied (by means of the TGA) under N_2 atmosphere from room temperature to 950°C with the heating rate of 10°C per minute. We can observe that the thermal decomposition ends at 600°C for the Zn(II) complex. There is no mass loss up to ≈ 250°C for confirming the absence of any crystalline water (solvent) molecules in the complexes. Zn(II) complex loses ≈ 99% of its weight *via* two thermal stages. The increasing weight after thermal decomposition temperature is definitely due to formation of Zinc oxide.

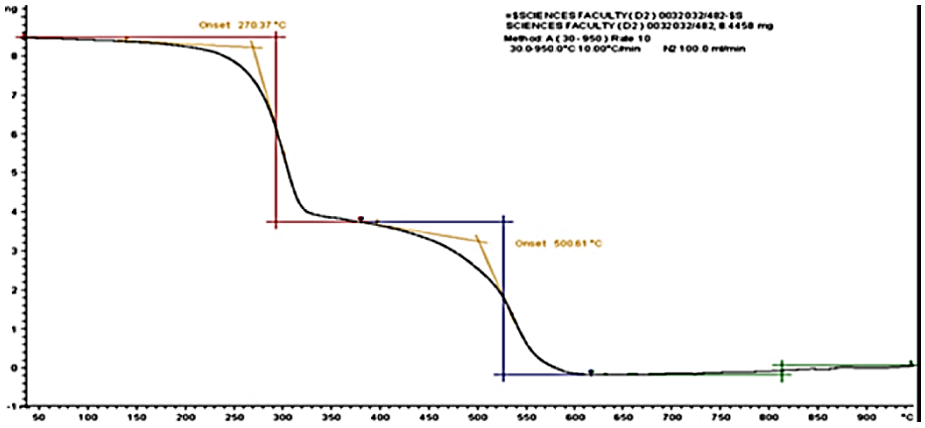

Fig. 4. TGA curve for Zn(II) complex.

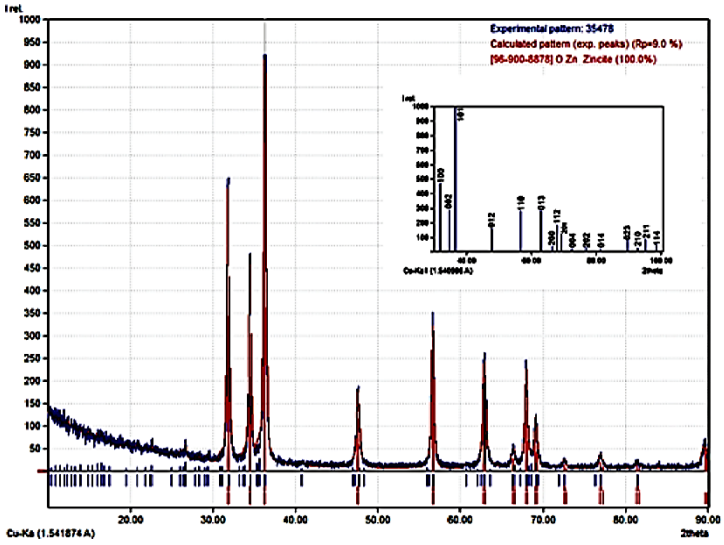

Fig. 5. XRD spectrum for Zinc oxide.

3.4. X-Ray Structural Analysis for the Oxides

The phase identification of crystalline structure of the nanoparticles was characterised by x-ray powder diffraction. The synthesized sample was analysed by the CuK_α x-ray diffractometer for confirming the presence of ZnO and identification of the structure.

Figure 5 shows the XRD patterns of ZnO nanoparticle synthesized. The different peaks are observed at $2\Theta = 31.94°$ (100), 34.55° (002),

36.45° (101), 47.65° (102), 56.75° (110), 62.95° (103), 66.45° (200), 68.10° (112) and 69.20° (201), which are indexed to the hexagonal wurtzite structure (COD Card No. 96-900-8878) (space group: $P63m$) with lattice constants $a = b = 3.2494$ Å and $c = 5.2054$ Å. The presence of the (100), (002) and (101) planes in XRD patterns indicates the formation of high purity of the ZnO nanoparticles. Further, no peaks due to impurities were observed. Strong intensity and narrow width of the ZnO diffraction peaks indicate that the resulting product was highly crystalline [18]. Average size of ZnO nanoparticles can be estimated using the Debye–Scherrer equation, which gives a relationship between peak broadening in XRD and particle size that is demonstrated by the following equation: $D_c = k\lambda/(\beta\cos\theta)$, where D_c is the crystal nanoparticle size, k is Scherrer's constant (0.89), λ is x-ray wavelength (0.15406 nm), β is the width of the XRD peak at half height, and θ is the Bragg diffraction angle [19]. By Match program [20] and using the Scherrer's equation, the average crystalline size of ZnO nanoparticles is found of 38.22 nm.

3.5. Energy Dispersive X-Ray Spectrometry (EDX)

The chemical stoichiometry of ZnO nanoparticle was investigated with EDX. This analysis was performed on three different areas randomly across the investigated sample to determine the Zinc and Oxygen ratio. Figure 6 shows the content of Zn, O and C elements in the sample. As detected, it is indicating the high purity of the synthesized ZnO. The Oxygen-to-Zinc weight ratio was found quantitatively from ≈ 1 to 4, and atomic ratio was found from ≈ 1 to 1, respectively, indicating the stoichiometric formation of ZnO, while 4% Carbon weight ratio attributed to EDX sample holder.

3.6. Scanning Electron Microscopy (SEM) Measurement

The SEM image of prepared nanoparticles is given in Fig. 7. The diameter of the nanoparticles is found to be in the range of 16–60 nm, and they are nearly spherical in shape.

4. CONCLUSION

In summary, we have synthesized ZnO nanoparticles using direct thermal decomposition method. The preparation process of ZnO nanoparticles is quite facile. XRD pattern indicates the formation of ZnO nanoparticles of pure hexagonal wurtzite structure with average particle size found to be of 38.22 nm. Here, we report a simple, green, low-cost, and reproducible process for the synthesis. In this

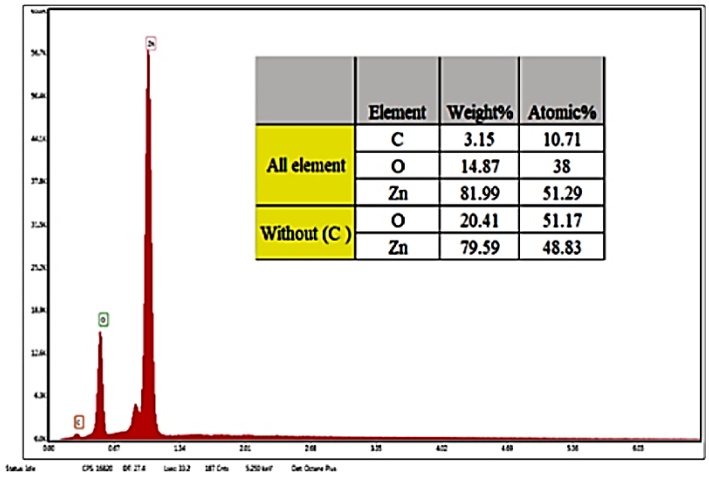

Fig. 6. Energy dispersive spectrum indicating the chemical composition of freshly prepared for ZnO nanoparticles.

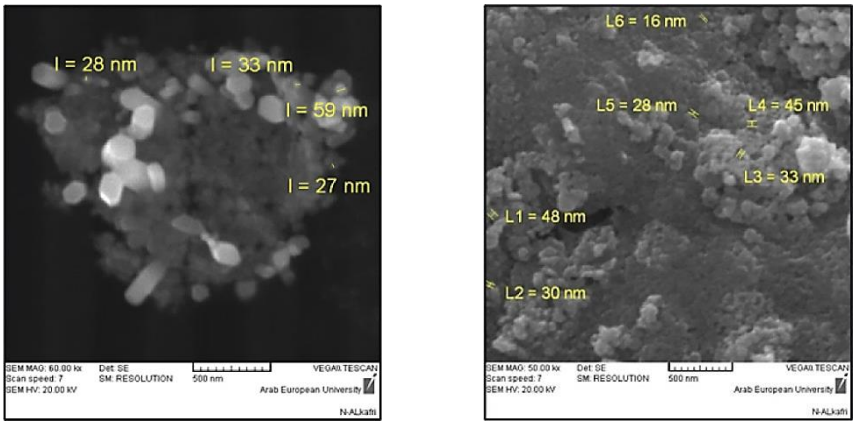

Fig. 7. SEM image of ZnO nanoparticles.

process, surfactant (C12-14-secondary alcohol ethoxylate) was used as both the medium and the stabilizing reagent, while polyvinylpyrrolidone (PVP) can serve as a surface stabilizer, growth modifier, and nanoparticle dispersant.

5. HIGHLIGHTS

The XRD pattern confirmed the crystalline nature of ZnO nanoparticles. As revealed from FT-IR pattern, the ZnO bonding and the functional groups responsible for reduction of ZnO nanoparticles

are presented. Structural morphology of ZnO nanoparticles was studied by SEM analysis.

COMPLIANCE WITH ETHICAL STANDARDS

This study was funded by Damascus University. Authors declares that they have no conflict of interest.

REFERENCES

1. L. J. Lauhon, M. S. Gudiksen, D. Wang, and C. M. Lieber, *Nature*, **420**, No. 6911: 57 (2002); doi:10.1038/nature01141
2. A.Weibel, R. Bouchet, P. Bouvier, and P. Knauth, *Acta Materialia*, **54**, No. 13: 3575 (2006).
3. M. Frietsch, F. Zudock, J. Goschnick, and M. Bruns, *Sen. and Act. B: Chem.*, **65**, Nos. 1–3: 379 (2000).
4. T. Kawano and H. Imai, *Crystal Growth & Design*, **6**, No. 4: 1054 (2006).
5. J. Tamaki, *Sensor Letters*, **3**, No. 2: 89 (2005).
6. M. Kurtz, J. Strunk, O. Hinrichsen, M. Muhler, K. Fink, B. Meyer, and C. Wöll, *Angewandte Chemie International Edition*, **44**, No. 18: 2790 (2005).
7. C. L. Yang, J. N. Wang, W. K. Ge, L. Guo, S. H. Yang, and D. Z. Shen, *Journal of Appl. Phys.*, **90**, No. 9: 4489 (2001).
8. M. Izaki, K. T. Mizuno, T. Shinagawa, M. Inaba, and A. Tasaka, *Journal of the Electrochemical Society*, **153**, No. 9: C668 (2006).
9. S. H. Lee, S. S. Lee, J. J. Choi, J. U. Jeon, and K. Ro, *Microsystem Technologies*, **11**, No. 6: 416 (2005).
10. H. Chang, M. Kao, C. Jwo, C. Kuo, Y. Yeh, and W. Tzeng, *Journal of Alloys and Compounds*, **504**, Suppl. 1: S376 (2010); https://doi.org/10.1016/j.jallcom.2010.04.127
11. S. J. Chen, X. T. Chen, Z. Xue, L. H. Li, and X. Z. You, *Journal of Crystal Growth*, **246**, Nos. 1–2: 169 (2002).
12. X. Liu, B. Geng, Q. Du, J. Ma, and X. Liu, *Materials Science and Engineering: A*, **448**, Nos. 1–2: 7 (2007).
13. M. Epifani, G. De, A. Licciulli, and L. Vasanelli, *Journal of Materials Chemistry*, **11**, No. 12: 3326 (2001).
14. C. Xu, Y. Liu, G. Xu, and G. Wang, *Materials Research Bulletin*, **37**, No. 14: 2365 (2002).
15. L. Gou and C. J. Murphy, *Nano Letters*, **3**, No. 2: 231 (2003).
16. A. D. Khalaji, *Journal of Cluster Science*, **24**, No. 1: 209 (2013).
17. S. Farhadi and J. Safabakhsh, *Journal of Alloys and Compounds*, **515**, No 1: 180 (2012).
18. D. Das, B. Nath, P. Phukon, and S. K. Dolui, *Colloids and Surfaces B: Biointerfaces*, **11**, No. 1: 556 (2013).
19. A. Janaki, E. Sailatha, and S. Gunasekaran, *Spectrochimica Acta. Part A: Molecular and Biomolecular Spectroscopy*, **144**, No. 2: 17 (2015).
20. *Match! - Phase Analysis using Powder Diffraction. Crystal Impact GbR* (Dr. H. Putz & Dr. K. Brandenburg GbR, Kreuzherrenstr. 102, D-53227 Bonn, Germany); http://www.crystalimpact.com/match